Supporting Information for:

Understanding the Amorphous Lithiation Pathway of the Type I Ba_8Ge_{43} Clathrate with Synchrotron X-ray Characterization

*Andrew Dopilka[1], Amanda Childs[2], Svilen Bobev[2], Candace K. Chan[1,3]**

1. Materials Science and Engineering, School for Engineering of Matter, Transport and Energy, Arizona State University, P.O. Box 876106, Tempe, AZ 85827
2. Department of Chemistry and Biochemistry, University of Delaware, Newark, DE 19716
3. Department of Heterogenous Catalysis, Max-Planck-Institut für Kohlenforschung, Kaiser-Wilhelm-Platz 1, 45470 Mülheim an der Ruhr, Germany

Corresponding author: *candace.chan@asu.edu

Table of Contents

Experimental Procedures

1.1. Synthesis of type I Ge clathrates

The synthesis of Ba_8Ge_{43} and $Ba_8Al_{16}Ge_{30}$ was prepared in a similar manner as described in our previous work.[1] Metals of Ba, and Al and Ge (commercial grade materials with stated purity 99.9% wt) were weighed in an Ar-filled glove box (controlled O_2 and moisture atmosphere). An extra amount (5%) of Ba was loaded since Ba is more volatile than other elements. The total weight of the starting materials was ca. 600 mg. Then, the materials were quickly transferred to the chamber of a custom-made arc-melter, which was evacuated to ca. 10^{-4} Torr and backfilled with high purity argon. After the initial melting, the formed ingot was taken out and turned over. The melting process was repeated three times to ensure good homogeneity. The ingot was hand ground in a mortar and pestle prior to electrochemical testing.

1.2. Electrochemical measurements

The clathrate powder was prepared into slurries by mixing the clathrate sample with 10 wt% carbon black (to serve as conducting additive) and 10 wt% polyvinylidene difluoride (PVDF) (to serve as binder) in N-methyl pyrrolidone (NMP) as solvent. Hand ground 100 mesh Ge powder (Sigma Aldrich 99.999%) was used to prepare electrodes for comparison to the clathrate samples. The slurries were stirred overnight and coated onto Cu foil current collectors using a Meyer rod, and then heated at 120 ^oC to remove the solvent. Electrodes were cut into circles 18 mm in diameter and typically had an area mass loading of 4-4.5 mg/cm^2. The clathrate composite electrodes were evaluated in pouch cells with Li metal as the counter electrode, Celgard 2500 as separator, and 1 M $LiPF_6$ in ethylene carbonate and ethyl methyl carbonate (3: 7 by vol) (LBC3015B, MTI) as electrolyte. Electrochemical testing was performed using a Biologic VMP3 galvanostat/potentiostat. Galvanostatic measurements were performed at 25 mA/g from 0.01 – 2.5 V vs. Li/Li^+. After the cell was lithiated to the desired composition, it was allowed to relax at open circuit for 5 hours prior to disassembly. To provide sufficient lithiated powder for

structural characterization, samples from 2-3 cells prepared and electrochemically lithiated in the same manner were combined.

1.3. Sample preparation for synchrotron measurements

After the electrochemical lithiation was complete, the pouch cell was taken into the argon-filled glovebox and opened. The electrode was then immersed in 10 mL of dimethyl carbonate for 30 seconds to wash off any excess battery electrolyte. After the electrode was dry, the lithiated powder was scraped off of the copper current collector using a knife. The extracted powder was then crushed in a mortar and pestle to break up any agglomeration. The powder was sealed in a 2 mL centrifuge tube and then sealed under argon in a polyfoil bag before shipping to the synchrotron facility.

1.4. Pair distribution function (PDF) analysis

Lithiated powders were loaded into 0.8 mm diameter borosilicate capillaries and sealed with wax and superglue inside an argon-filled glovebox, while pristine powders were loaded into the capillaries in ambient conditions. PDF measurements were performed at the Diamond Light Source (Didcot, United Kingdom) at the I15-I dedicated PDF beamline with 76 keV X-rays (wavelength of 0.161669 Å) and 2D PerkinElmer image plate detectors. The detector geometry allowed collection of total scattering data to Q = 30 $Å^{-1}$. *Ex situ* PDF measurements were carried out at room temperature. The *in situ* PDF heating measurements were carried out from 300 – 450 K (temperature interval of 10 K) using an Oxford Instruments Cryojet 5. After reaching each hold temperature, there was a 1.5 min equilibration period and then the scattering data were collected with a 10 minute collection time. For the $Li_{3.75}Ge$ heating experiments, a 5 minute collection time was used due to time constraints.

PDFs were generated from the total scattering data using PDFgetX3[2] within the xPDFsuite software package,[3] wherein the measured total scattering intensities, $I(Q)$, are corrected to obtain the coherent scattering, $I_c(Q)$ and transformed into the structure function, $S(Q)$, according to equation 1,[2]

$$S(Q) = \frac{I_c(Q) - \langle f(Q)^2 \rangle + \langle f(Q) \rangle^2}{\langle f(Q) \rangle^2} \quad (1)$$

where $f(Q)$ is the atomic scattering factor, which is averaged over all atom types in the sample. The PDF, $G(r)$, is obtained from the Fourier transform of $S(Q)$ as shown in equation 2:

$$G(r) = \frac{2}{\pi} \int_{Q_{min}}^{Q_{max}} Q[S(Q) - 1] \sin(Qr)\, dQ \quad (2)$$

To generate the PDFs, the following parameters were used: Q_{min} = 0.5 Å^{-1}, Q_{max} = 25 Å,$^{-1}$ r_{step} = 0.1 Å, and r_{poly}= 0.9. The nominal composition for lithiated samples was obtained from the charge passed during the electrochemical measurements.

PDF refinements were carried out using PDFgui[4]. No attempts were made to consider the presence of binder, carbon black, or SEI components in the samples. Previous reports have shown that these components add negligible contribution to the PDF data.[5] PDF refinements were performed using Q_{damp} = 0.0247 and Q_{broad} = 0.0151 (obtained from refinement of a NIST Si standard). To refine a PDF pattern, the major phase of the pattern was first selected and then the scale factor and lattice parameter were refined. Then, the atomic displacement parameters (ADP) for each element (initially set to 0.03 Å^2) and the linear atomic scale factor (*delta1*) were allowed to be refined. If this resulted in an insufficient fit, possible secondary phases were added and refined in a similar way. In some cases, the Li ADP refined to very large values (0.5 – 1 Å^2). If this occurred, the Li ADP was fixed to a lower value. Unphysical ADPs for Li have been reported previously and is an indication of disorder/partial occupancy or atomic substitution[6].

The refinements were conducted using the following structures for the fittings: Ba_8Ge_{43} ($Pm\bar{3}m$, ICSD-97480)[7], α-Ge ($Fd\bar{3}m$, ICSD-44841)[8], Li_9Ge_4 (*Cmcm*, ICSD-25308)[9], Li_7Ge_2 (*Cmmm*, ICSD-42063)[10], $Li_{15}Ge_4$ ($I\bar{4}3d$, ICSD-43235)[11], and Li_7Ge_3 ($P3_212$), Li_5Ge_2 ($R\bar{3}m$), and $Li_{13}Ge_5$ ($P\bar{3}m1$) (predicted from first principles calculations by Morris et. al[12]).

1.5. Powder X-ray diffraction (XRD)

Synchrotron XRD was performed at the P02.1 Powder Diffraction and Total Scattering Beamline at PETRA III at the Deutsches Elektronen-Synchrotron (DESY) with 60 keV X-rays at a wavelength of 0.20733 Å. A Perkin Elmer XRD1621 was used as the X-ray detector. The lithiated samples were loaded into 0.8 mm borosilicate capillaries in an argon-filled glovebox and sealed with wax. *In situ* heating experiments were conducted in borosilicate capillaries and heated with an Oxford Cryostream cooler. For the *in situ* measurements, 3 scans were taken every 2 minutes with a total hold time of 6 minutes at the temperature. A temperature interval of 20 K was used starting at 300 K and going to 480 K.

Rietveld refinement of the XRD patterns was performed with Jana2006[13]. The peak shapes were described by the pseudo-Voigt function, background fit with Legendre polynomials, and atomic displacement parameters (ADP) were modeled as isotropic. In some cases, the Li ADP refined to very large values (0.5 – 1 $Å^2$). If this occurred, the Li ADP was fixed to a lower value. Unphysical ADP for Li have been reported previously and is an indication of disorder/partial occupancy or atomic substitution[6].

Laboratory powder X-ray diffraction was performed with a Bruker D8 diffractometer with Cu X-rays operated at 40 kV and 40 mA with standard Bragg-Brentano diffraction geometry. For air-sensitive samples, the sample was covered with a Kapton film in an argon-filled glovebox prior to diffraction measurements. The Kapton film resulted in a broad amorphous background from $15 < 2\theta < 25$.

Obtained XRD patterns were compared to the same reference patterns indicated in the previous section, as well as the following: LiGe (*I*4$_1$/*a*, ICSD-42062)[14], Ba_2LiGe_3 (*Fddd*, ICSD-404705)[15], Li_4Ge_1 (*Cmcm*, ICSD-427231)[16], $Li_{17}Ge_4$ (*F*$\bar{4}$3*m*, ICSD-427232)[16].

1.6. Scanning electron microscopy

Scanning electron microscopy (SEM) imaging was performed using an XL30 ESEM-FEG microscope and a 20 kV electron beam. The electrodes were cut from copper foil and mounted on SEM stubs with carbon tape

Supporting Tables

Table S1. The measured voltages and corresponding capacity for each sample after electrochemical lithiation to different Li/Ge ratios.

Electrode	# of Li inserted per Ge atom	Voltage (V vs. Li/Li^+)	Capacity (mAh/g)
Ba_8Ge_{43}	1.75	0.175	478
	2.75	0.11	752
	3.75	0.01	1025
α-Ge	1.75	0.28	647
	2.75	0.17	1017
	3.75	0.01	1386

Table S2. Refined atomic positions, lattice parameters, and atomic displacement parameters for the $Li_{1.75}Ge$ sample. The refinement plot can be found in Figure S2a.

Ge	$Fd\bar{3}m$	**Lattice Parameter:**	**5.65735(8) Å**			
Atom	**Site**	**x/a**	**y/b**	**z/c**	**Occ.**	**U_{iso} (Å^2)**
Ge1	8b	0	0	0	1	0.0071(3)
Li_5Ge_2	$R\bar{3}m$	**Lattice Parameter:**	**a = 4.46774(18) Å**	**c = 18.3973(14) Å**		
Atom	**Site**	**x/a**	**y/b**	**z/c**	**Occ.**	**U_{iso} (Å^2)**
Li1	3a	0	0	1/2	1	0.05*
Li2	6c	0	0	0.350712	1	0.05*
Li3	6c	0	0	0.191734	1	0.05*
Ge1	6c	0	0	0.06795(11)	1	0.0112(7)

**The atomic displacement parameters for Li were fixed to 0.05 due to refining to unphysical values.*

Table S3. Refined atomic positions, lattice parameters, and atomic displacement parameters for the $Li_{3.75}Ge$ sample. The refinement plot can be found in Figure S2b.

$Li_{15}Ge_4$	$I\bar{4}3d$	**Lattice Parameter:**	**10.7763(4) Å**			
Atom	**Site**	**x/a**	**y/b**	**z/c**	**Occ.**	**U_{iso} (Å^2)**
Li1	48e	0.0349(17)	0.3727(13)	0.1515(13)	1	0.008(4)
Li2	12a	3/8	0	1/4	1	0.03*
Ge1	16c	0.20975(10)	x	x	1	0.0168(6)

**The atomic displacement parameters for Li were fixed to 0.03 due to refining to unphysical values.*

Table S4. PDFgui refinement parameters for pristine α-Ge and the $Li_{1.75}Ge$ sample fit to different phase combinations. Refinement plots for the pristine α-Ge sample and the $Li_{1.75}Ge$ sample refined to the structure of α-Ge and Li_5Ge_2 are presented in Figure S3ab.

	Pristine α-Ge	**$Li_{1.75}Ge$**		**$Li_{1.75}Ge$**		**$Li_{1.75}Ge$**	
Phase	Ge $Fd\bar{3}m$	Ge $Fd\bar{3}m$	Li_7Ge_3 $P3_212$	Ge $Fd\bar{3}m$	Li_5Ge_2 $R\bar{3}m$	Ge $Fd\bar{3}m$	Li_9Ge_4 $Cmcm$
Mol Fraction	1	0.096	0.904	0.094	0.906	0.093	0.907
Lattice Parameters (Å)	a= 5.655	a = 5.652	a = 7.723 c = 18.470	a = 5.652	a = 4.464 c = 18.435	a = 5.649	a = 4.453 b = 7.700 c = 24.808
Delta 1	1.937	1.724	2.397	2.444	1.045	1.748	2.419
ADP*	0.008	Ge: 0.011	Li: 0.204 Ge: 0.022	Ge: 0.011	Li: 0.280 Ge: 0.027	Ge: 0.0086	Li: 0.129 Ge: 0.031
R_w	0.082	0.197		0.191		0.229	

**Atomic displacement parameters (U_{11}= U_{22}= U_{33}, Å^2)*

Table S5. PDFgui refinement parameters for $Li_{2.75}Ge$ sample fit to different phase combinations. Plot of the sample refined with $Li_{13}Ge_5$ and Li_7Ge_2 is presented in Figure S3c.

	$Li_{2.75}Ge$		**$Li_{2.75}Ge$**	**$Li_{2.75}Ge$**
Phase	$Li_{13}Ge_5$ $P\bar{3}m1$	Li_7Ge_2 *Cmmm*	Li_7Ge_3 $P3_212$	Li_5Ge_2 $R\bar{3}m$
Mol Fraction	0.643	0.357	1	1
Lattice Parameters (Å)	a = 4.452 c = 16.122	a = 9.106 b = 13.233 c = 4.532	a = 7.735 c = 18.678	a = 4.470 c = 18.645
Delta 1	1.977	1.856	2.334	2.334
ADP*	Li: 0.086 Ge: 0.016	Li: 0.03** Ge: 0.018	Li: 0.062 Ge: 0.021	Li: 0.083 Ge: 0.023
R_w	0.195		0.255	0.268

**Atomic displacement parameters (U_{11}= U_{22}= U_{33}, Å^2)*
*** Note: Refinement of the ADPs for Li in the Li_7Ge_2 phase resulted in unreasonably high values so it was fixed at 0.03.*

Table S6. PDFgui refinement parameters for $Li_{3.75}Ge$ sample fit to different phase combinations. Plot of the sample refined with $Li_{15}Ge_4$ and Li_7Ge_3 is presented in Figure S3d.

	$Li_{3.75}Ge$	**$Li_{3.75}Ge$**		**$Li_{3.75}Ge$**	
Phase	$Li_{15}Ge_4$ $I\bar{4}3d$	$Li_{15}Ge_4$ $I\bar{4}3d$	Li_7Ge_3 $P3_212$	$Li_{15}Ge_4$ $I\bar{4}3d$	Li_5Ge_2 $R\bar{3}m$
Mol Fraction	1	0.857	0.143	0.862	0.138
Lattice Parameters (Å)	a = 10.784	a = 10.763	a = 7.728 c = 18.814	a = 10.763	a = 4.471 c = 18.751
Delta 1	0.763	1.724	1.929	1.799	1.045
ADP*	Li: 0.064 Ge: 0.016	Li: 0.105 Ge: 0.013	Li: 0.045 Ge: 0.015	Li: 0.107 Ge: 0.013	Li: 0.044 Ge: 0.016
R_w	0.229	0.118		0.127	

**Atomic displacement parameters (U_{11}= U_{22}= U_{33}, Å^2)*

Table S7. PDFgui refinement parameters for the pristine Ba_8Ge_{43} and $Li_{1.75}Ba_{0.19}Ge$ PDF plots in Figure S6.

	Pristine Ba_8Ge_{43}		**$Li_{1.75}Ba_{0.19}Ge$**	**$Li_{1.75}Ba_{0.19}Ge$ (10 < r < 30 Å)**
Phase	Ba_8Ge_{43} $Pm\bar{3}n$	Ge $Fd\bar{3}m$	Ba_8Ge_{43} $Pm\bar{3}n$	Ba_8Ge_{43} $Pm\bar{3}n$
Mol Fraction	0.956	0.044	1	1
Lattice Parameter (Å)	a = 10.658	a = 5.652	a = 10.652	a = 10.646
Delta 1	2.285	n/a	2.432	2.432
ADP*	Ba: 0.050 Ge: 0.027	Ge: 0.007	Ba: 0.027 Ge: 0.025	Ba: 0.022 Ge: 0.022
R_w	0.130		0.587	0.290

**Atomic displacement parameters (U_{11}= U_{22}= U_{33}, Å^2)*

Table S8. PDFgui refinement parameters for pristine $Ba_8Al_{16}Ge_{30}$ and $Li_{1.9}Ba_{0.17}Al_{0.35}Ge_{0.65}$ PDF plots in Figure S8bc.

	Pristine $Ba_8Al_{16}Ge_{30}$	**$Li_{1.9}Ba_{0.17}Al_{0.35}Ge_{0.65}$**
Phase	$Ba_8Al_{16}Ge_{30}$ $Pm\bar{3}n$	$Ba_8Al_{16}Ge_{30}$ $Pm\bar{3}n$
Mol Fraction	1	1
Lattice Parameter (Å)	a = 10.854	a = 10.836
Delta 1	1.489	2.0
ADP*	Ba: 0.05 Ge/Al: 0.014	Ba: 0.023 Ge/Al: 0.01
R_w	0.095	0.674

**Atomic displacement parameters (U_{11}= U_{22}= U_{33}, Å^2)*

Table S9. PDFgui refinement parameters for PDFs of $Li_{2.75}Ba_{0.19}Ge$ and $Li_{3.75}Ba_{0.19}Ge$ after heating to 450 K and 420 K, respectively. Plots of these refinements can be found in Figure S11.

	$Li_{2.75}Ba_{0.19}Ge$	**$Li_{2.75}Ba_{0.19}Ge$ (6 < r < 30 Å)**	**$Li_{3.75}Ba_{0.19}Ge$**
Phase	Li_7Ge_2 *Cmmm*	Li_7Ge_2 *Cmmm*	$Li_{15}Ge_4$ $I\bar{4}3d$
Mol Fraction	1	1	1
Lattice Parameters (Å)	a = 9.315 b = 13.154 c = 4.561	a = 9.317 b = 13.174 c = 4.55	a = 10.826
Delta 1	2.569	2.569	1.040
ADP*	Li: 0.1** Ge: 0.027	Li: 0.1** Ge: 0.025	Li: 0.1** Ge: 0.018
R_w	0.550	0.286	0.389

**Atomic displacement parameters (U_{11}= U_{22}= U_{33}, $Å^2$)*

**Refinement of the ADP for Li in both cases resulted in unreasonably high values so it was fixed.*

Supporting Figures

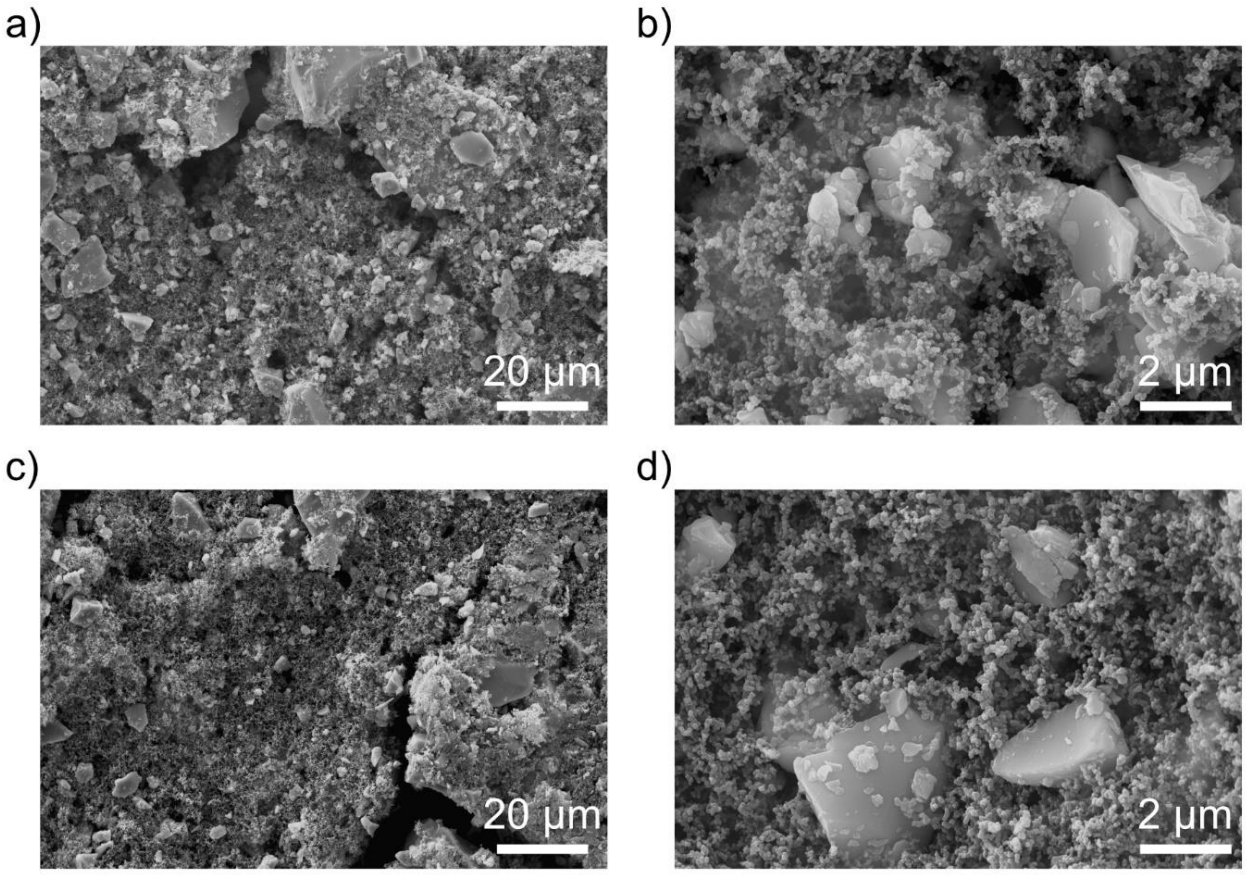

Figure S1. SEM images of the **(a,b)** Ba_8Ge_{43} and **(c,d)** α-Ge electrodes prior to electrochemical cycling. The small, nanosized particles are the carbon black conducting additive used to improve electronic conductivity throughout the composite electrode.

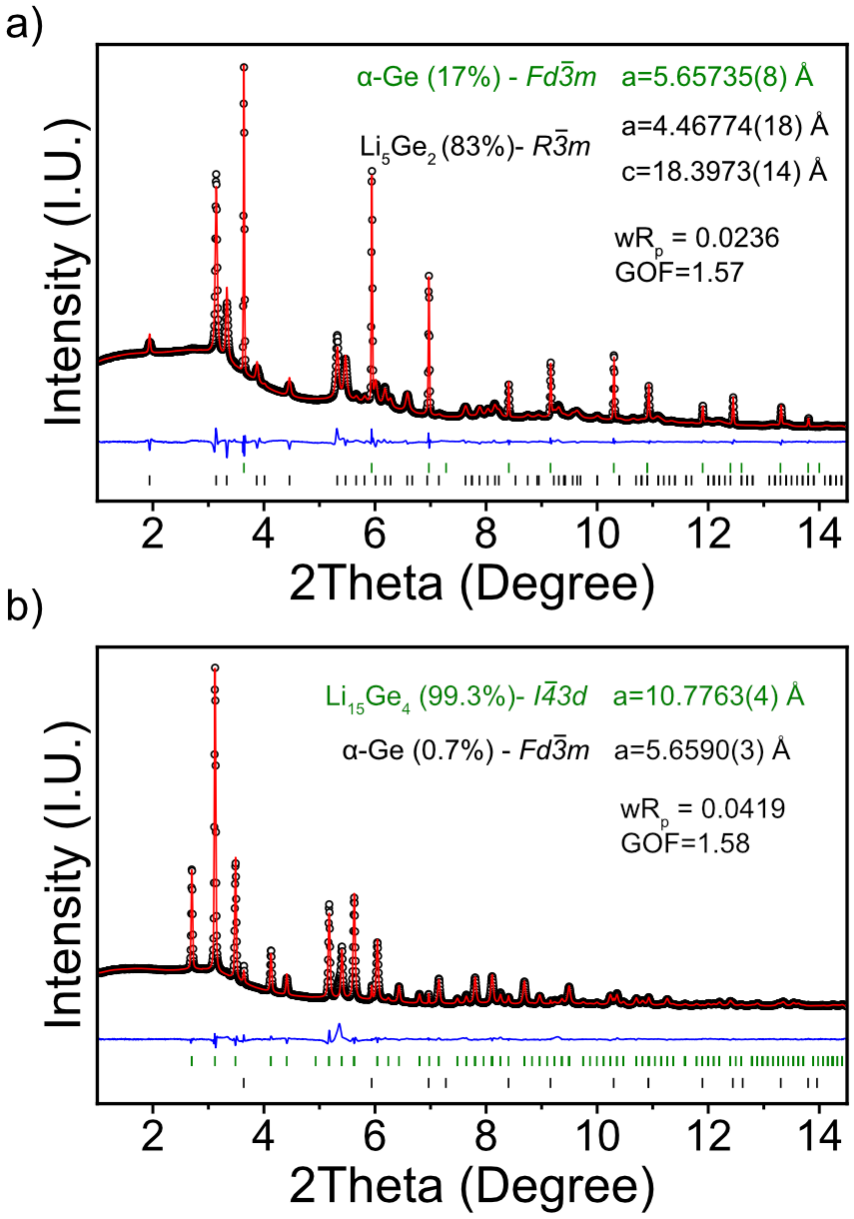

Figure S2. Rietveld refinements of the PXRD patterns of the (a) $Li_{1.75}Ge$ and (b) $Li_{3.75}Ge$ samples. The black circles represent the experimental pattern, the red curve represents the calculated pattern, and the blue curve represents the difference curve. The phase fractions are in mol%. The refined atomic positions, occupancies, and atomic displacement parameters can be found in **Table S2-3**.

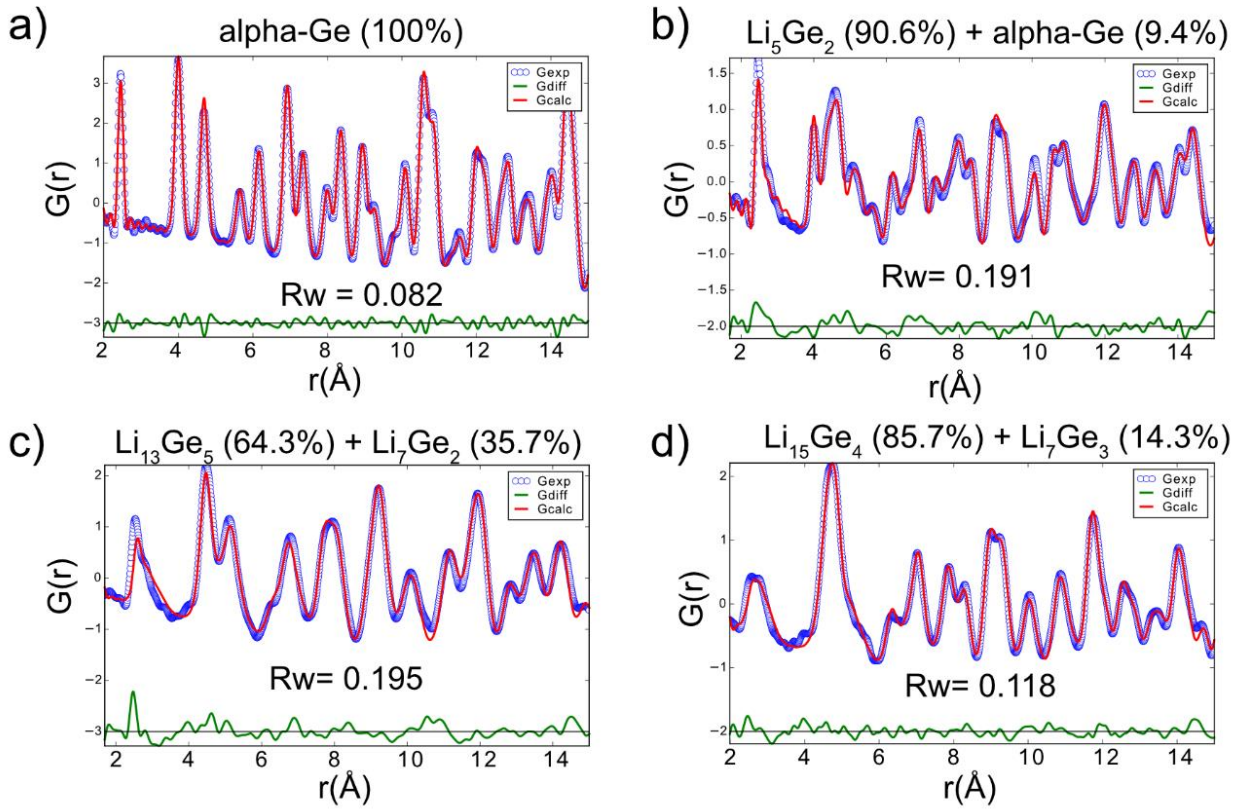

Figure S3. Refinements of the α-Ge PDF patterns at compositions of (a) pristine α-Ge (b) $Li_{1.75}Ge$, (c) $Li_{2.75}Ge$ and (d) $Li_{3.75}Ge$. Phase amounts indicated in mol%. The sources for the reference structures are included in Section 1.4 of the Supporting Information.

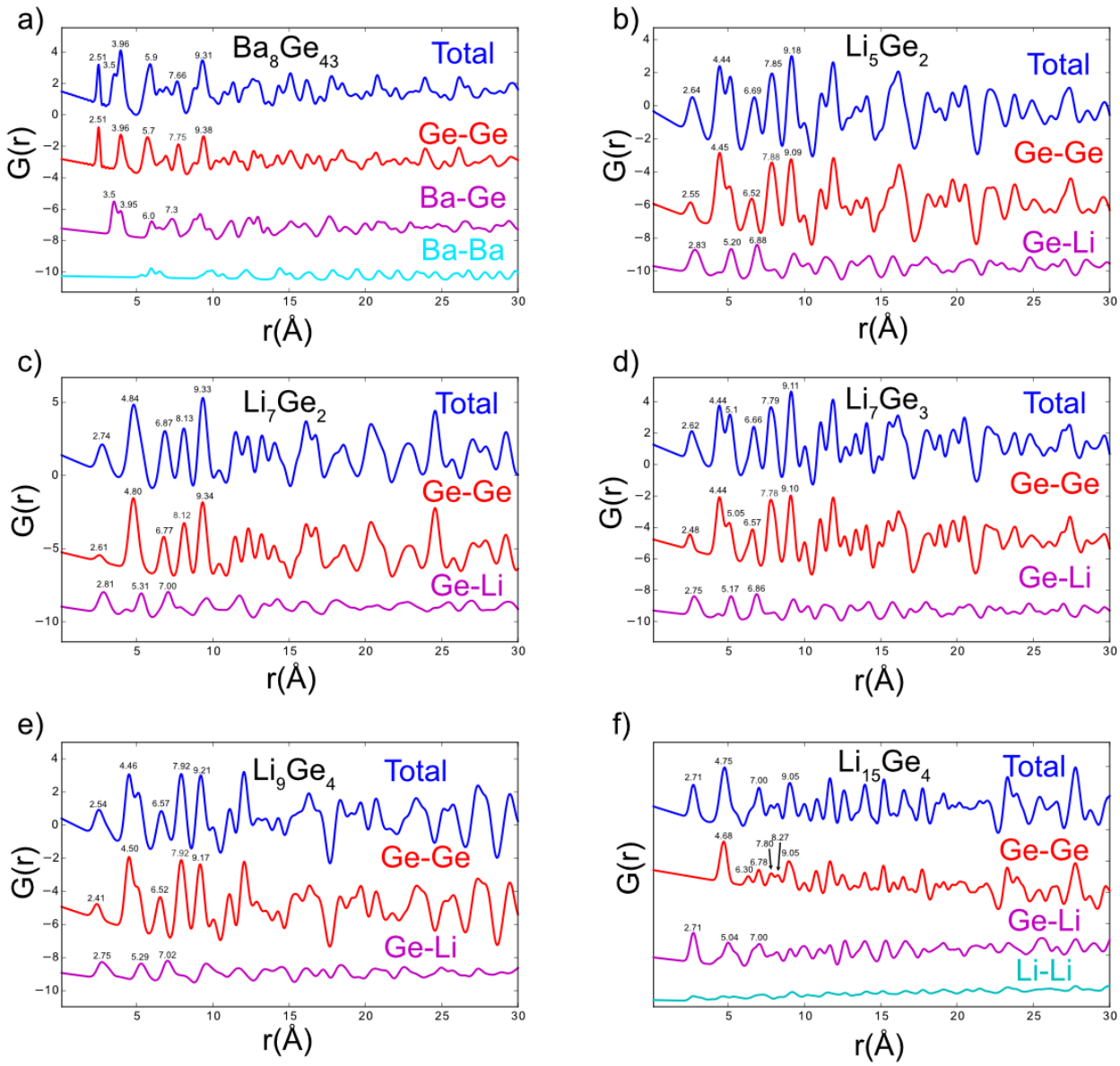

Figure S4. Calculated total and partial PDF patterns for (a) Ba_8Ge_{43}, (b) Li_5Ge_2, (c) Li_7Ge_2, (d) Li_7Ge_3, (e) Li_9Ge_4, and (f) $Li_{15}Ge_4$. The sources for the reference structures are included in Section 1.4 of the Supporting Information except for the structure of Ba_8Ge_{43}, which came from our previous study.[1]

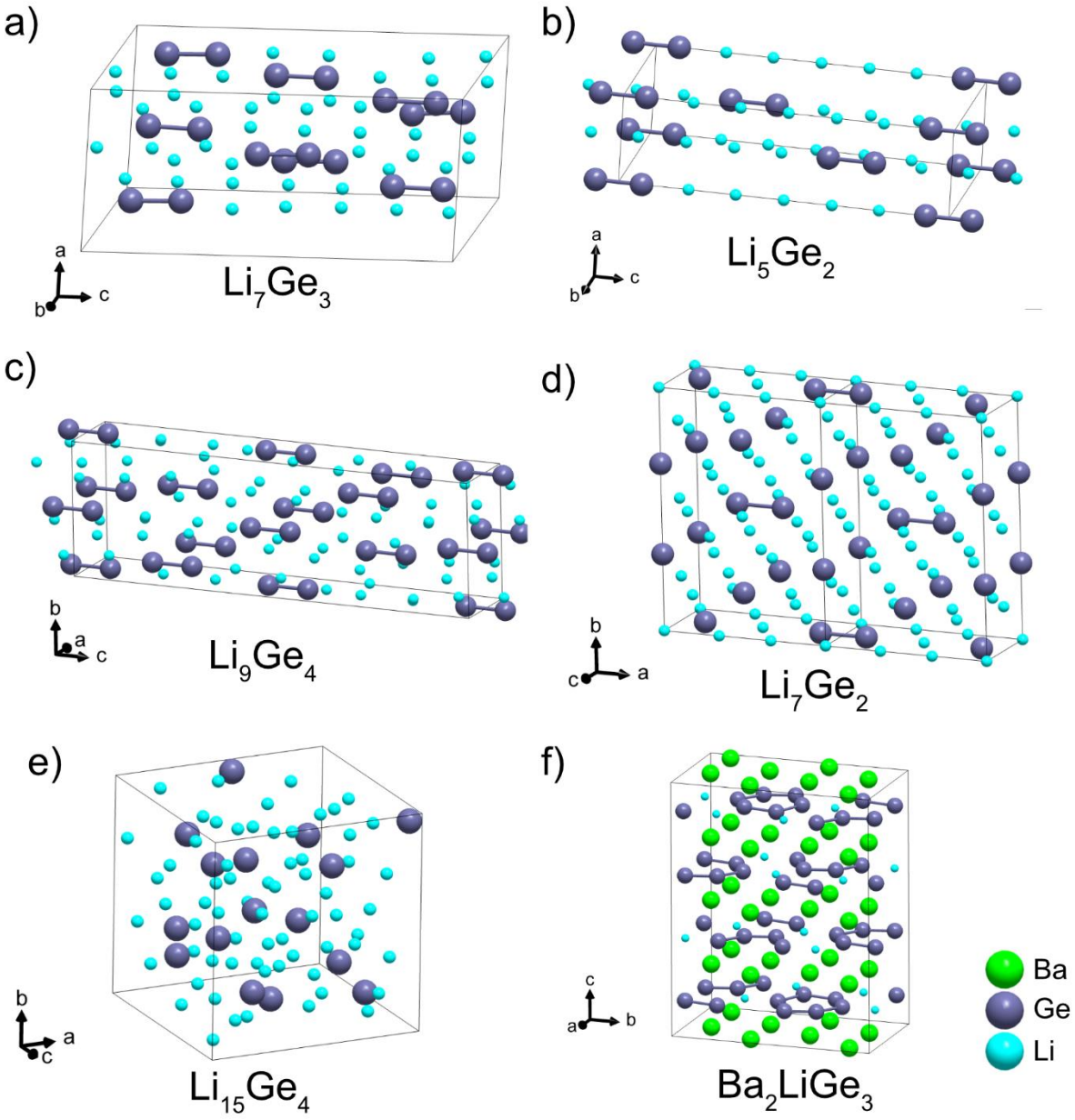

Figure S5. Crystal structures of (a) Li_7Ge_3, (b) Li_5Ge_2, (c) Li_9Ge_4, (d) Li_7Ge_2 (e) $Li_{15}Ge_4$, and (f) Ba_2LiGe_3. The sources for the reference structures are included in Section 1.4 and 1.5 of the Supporting Information.

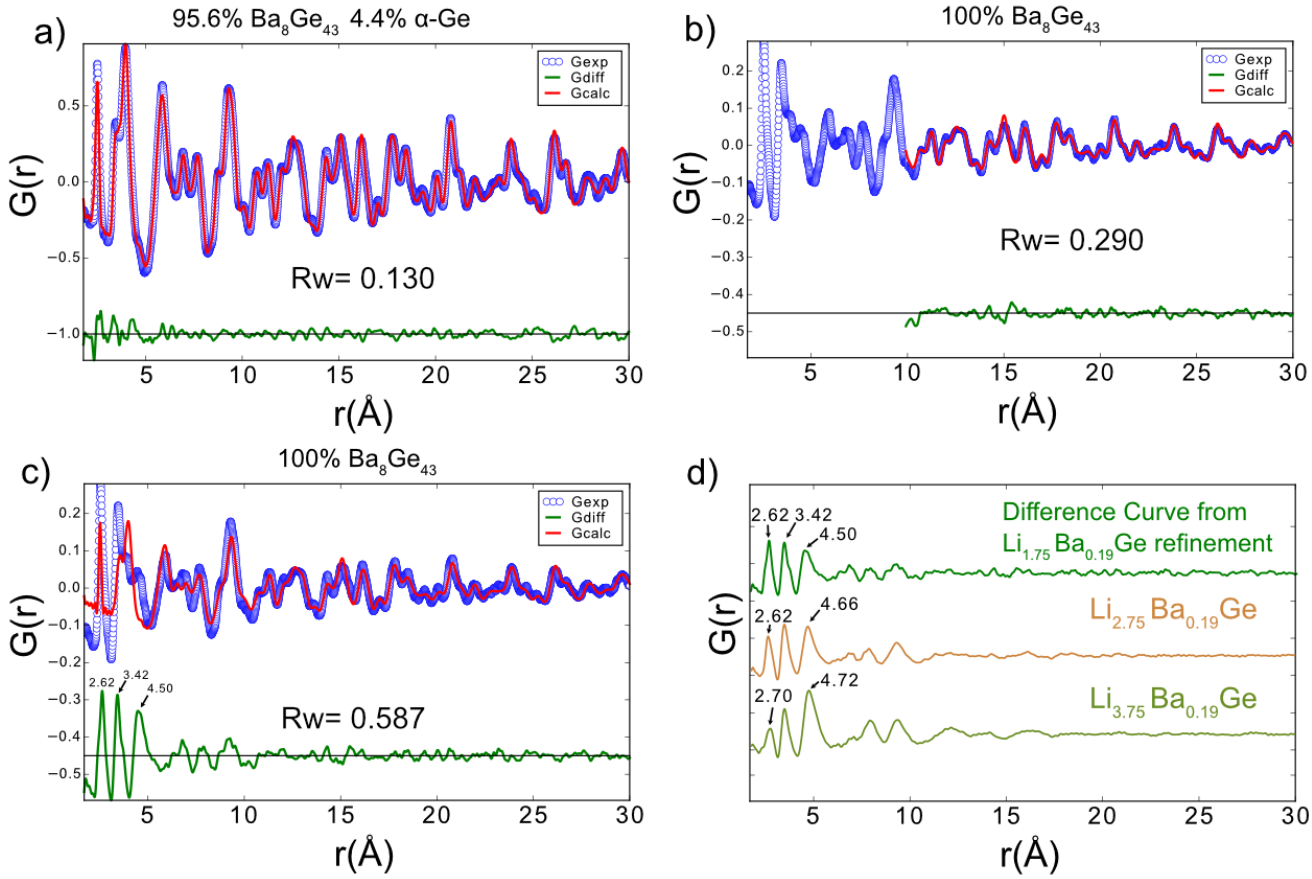

Figure S6. PDF refinements for (a) pristine Ba_8Ge_{43}, (b) Ba_8Ge_{43} after lithiation to a composition of $Li_{1.75}Ba_{0.19}Ge$ and (c) $Li_{1.75}Ba_{0.19}Ge$ (fit range restricted to 10 – 30 Å). (d) Comparison of the amorphous phase from the difference curve of the refinement for $Li_{1.75}Ba_{0.19}Ge$ in (c) with the PDFs of $Li_{2.75}Ba_{0.19}Ge$ and $Li_{3.75}Ba_{0.19}Ge$ (y-offset for clarity). The sources for the reference structures are included in Section 1.4 of the Supporting Information.

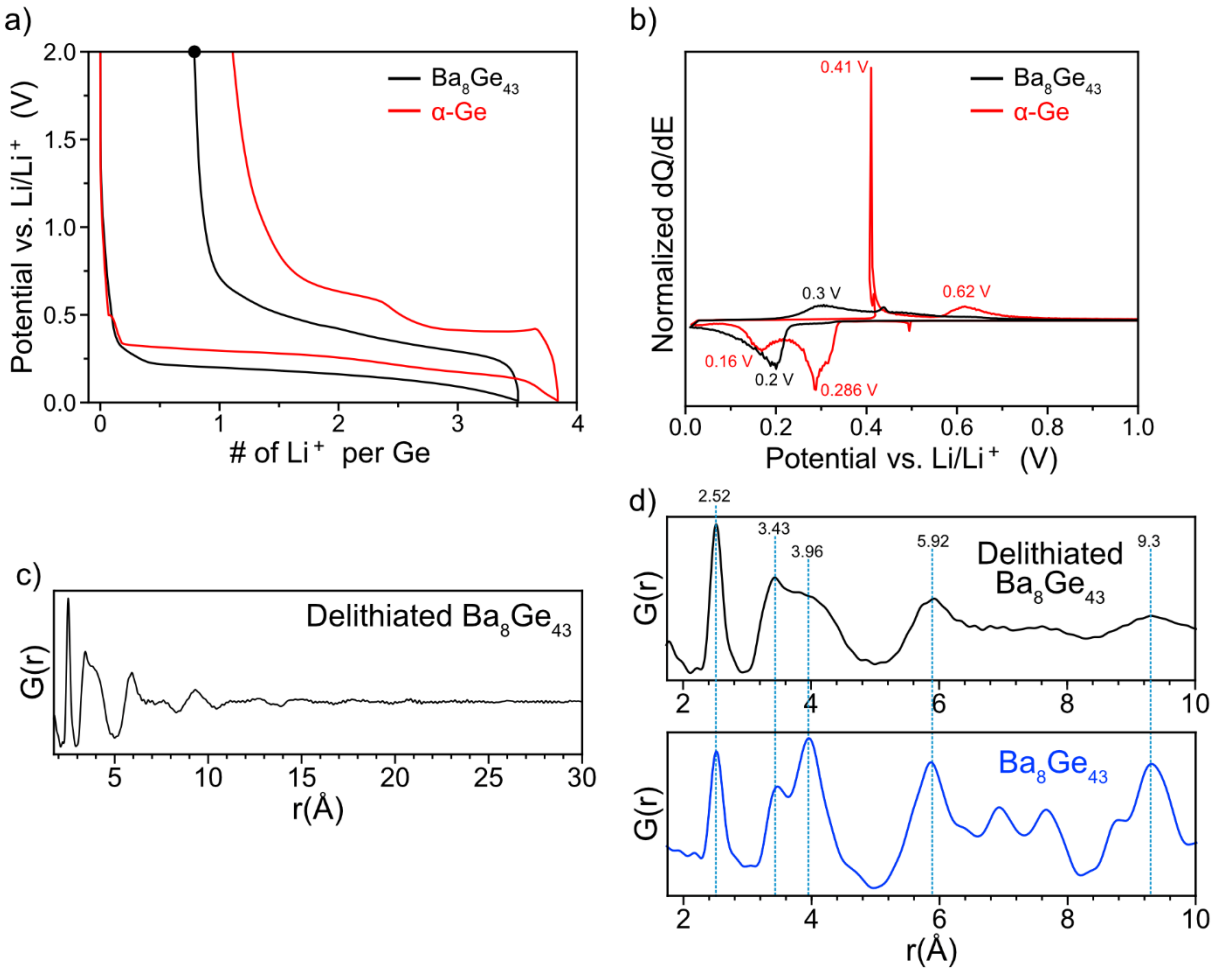

Figure S7. (a) Voltage profile of the lithiation and delithiation of Ba_8Ge_{43} and α-Ge using 25 mA/g; the # of Li^+ is referenced to the amount of Ge atoms in each compound. (b) Corresponding dQ/dE plot of the voltage profiles. (c) PDF plot of the Ba_8Ge_{43} after one full lithiation/delthiation cycle ("delithiated Ba_8Ge_{43}") taken from the point indicated by the black dot in the voltage profile in (a). (d) Comparison of PDFs from delithiated Ba_8Ge_{43} (amorphous) and the crystalline Ba_8Ge_{43}. The position of the peaks in the PDFs are similar, suggesting that the delithiated Ba_8Ge_{43} might have a similar local structure as the crystalline Ba_8Ge_{43}.

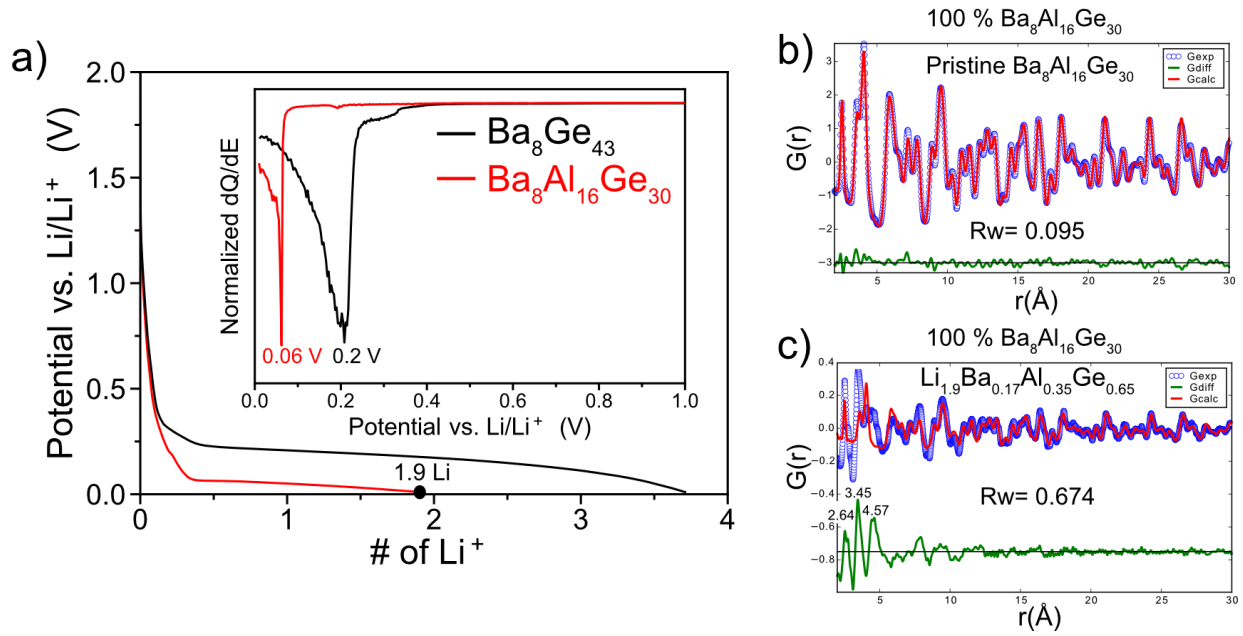

Figure S8. (a) Voltage profile and corresponding dQ/dE plot of the lithiation of Ba_8Ge_{43} and $Ba_8Al_{16}Ge_{30}$ using 25 mA/g; the # of Li^+ is referenced to the amount of (Al + Ge) atoms in each compound. (b) PDF refinement of the pristine $Ba_8Al_{16}Ge_{30}$ clathrate, using structure from ref.[1] (c) PDF refinement of the lithiated $Ba_8Al_{16}Ge_{30}$ ($Li_{1.9}Ba_{0.17}Al_{0.35}Ge_{0.65}$) to the $Ba_8Al_{16}Ge_{30}$ structure from ref.[1] The difference curve reveals the presence of an amorphous phase with similar correlation positions as those found in $Li_{1.75}Ba_{0.19}Ge$ (**Figure S6c**).

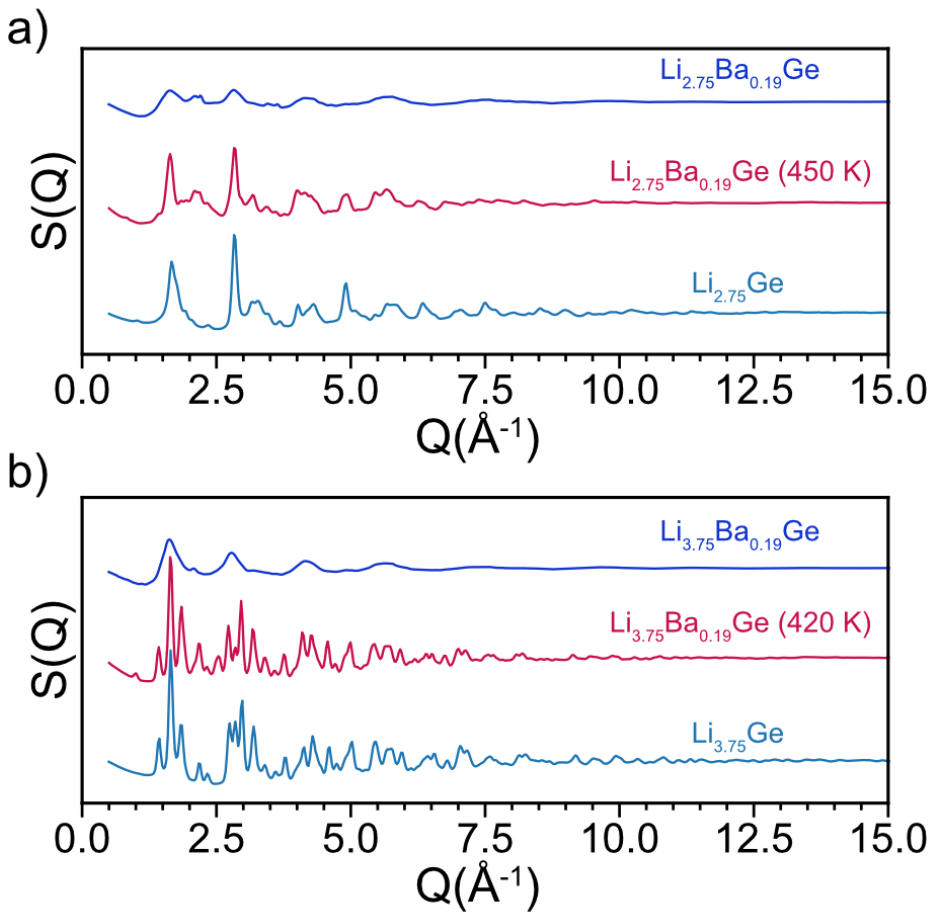

Figure S9. Comparison of total scattering structure function, $S(Q)$, with intensities normalized by the average scattering factors and corrected by a polynomial fit of (a) $Li_{2.75}Ba_{0.19}Ge$: unheated (blue), heated to 450 K (pink), and lithiated α-Ge (light blue); (b) $Li_{3.75}Ba_{0.19}Ge$: unheated (blue), heated to 420 K (pink), and lithiated α-Ge (light blue).

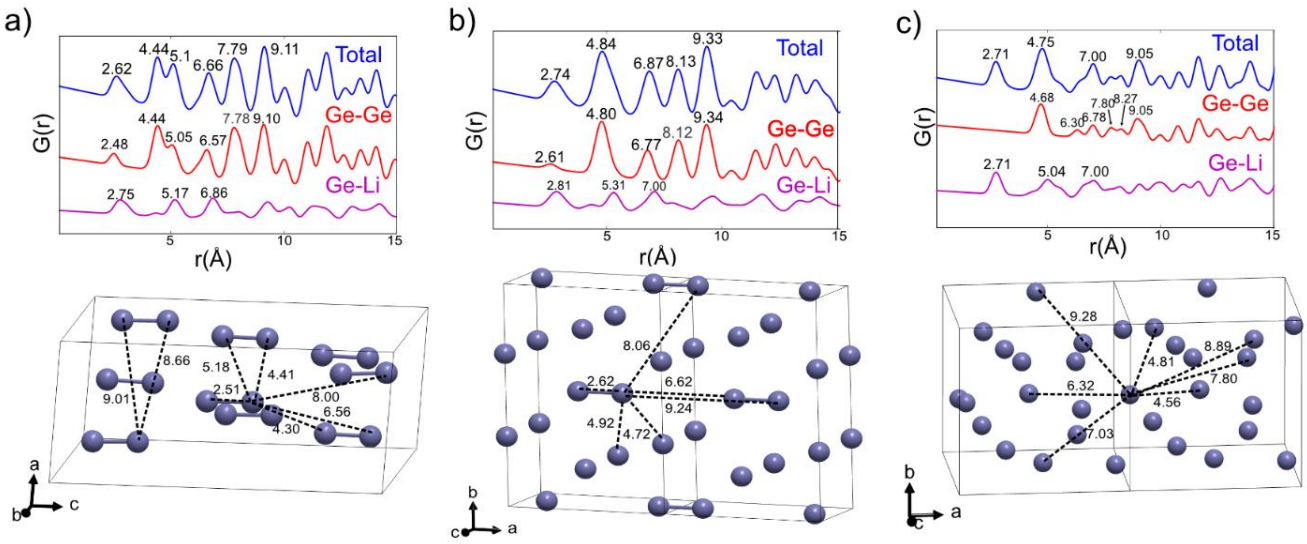

Figure S10. Assignment of Ge-Ge correlation distances found in the calculated PDF to distances between Ge atoms for (a) Li_7Ge_3 (b) Li_7Ge_2 and (c) $Li_{15}Ge_4$. Note that this is not an exhaustive assignment of the atomic correlations but serves to give an idea of the types of atom-atom distances corresponding to the correlations in the PDFs. The sources for the reference structures are included in Section 1.4 of the Supporting Information.

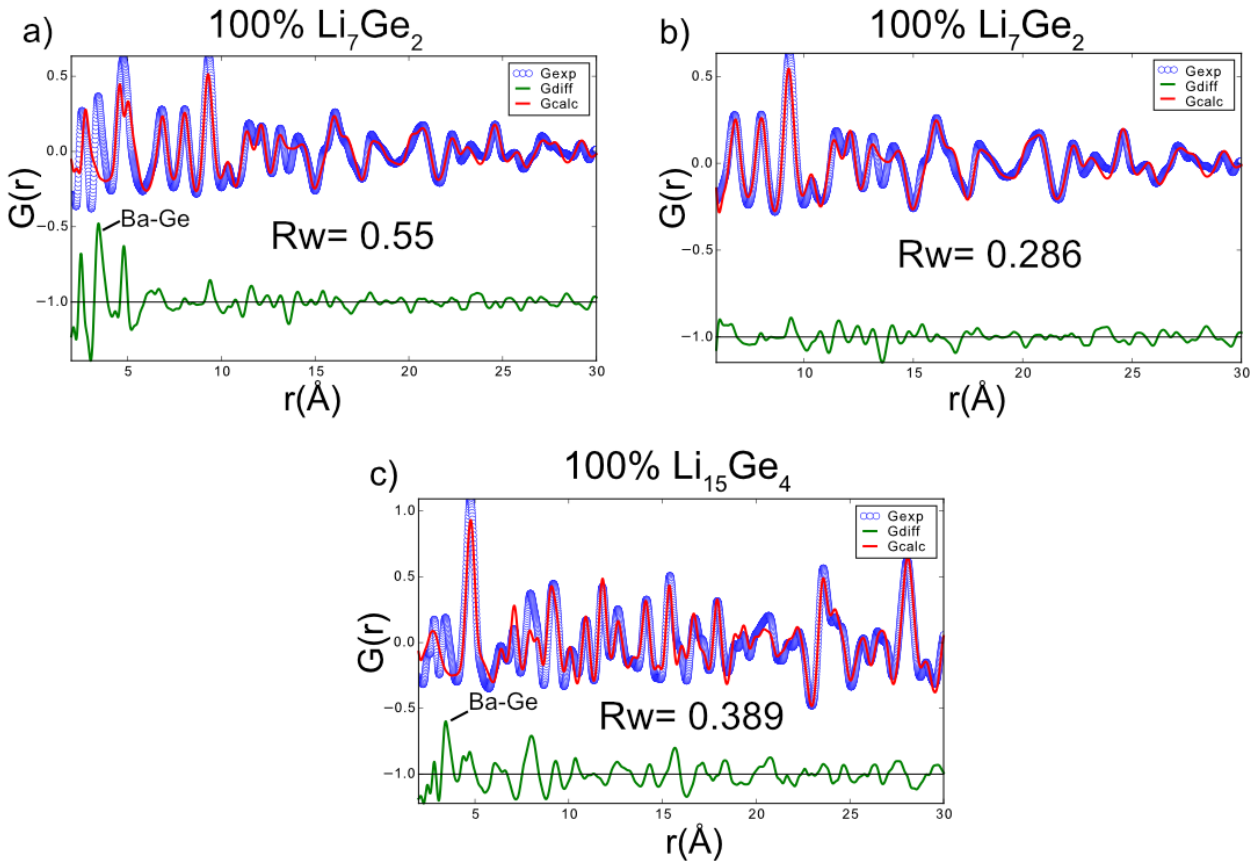

Figure S11. Refinements of the PDF from $Li_{2.75}Ba_{0.19}Ge$ after heating to 450 K, fit to Li_7Ge_2 (a) from 2 – 30 Å, and (b) from 6 – 30 Å. (c) Refinement of the PDF for $Li_{3.75}Ba_{0.19}Ge$ heated to 420 K, fit to $Li_{15}Ge_4$. The sources for the reference structures are included in Section 1.4 of the Supporting Information.

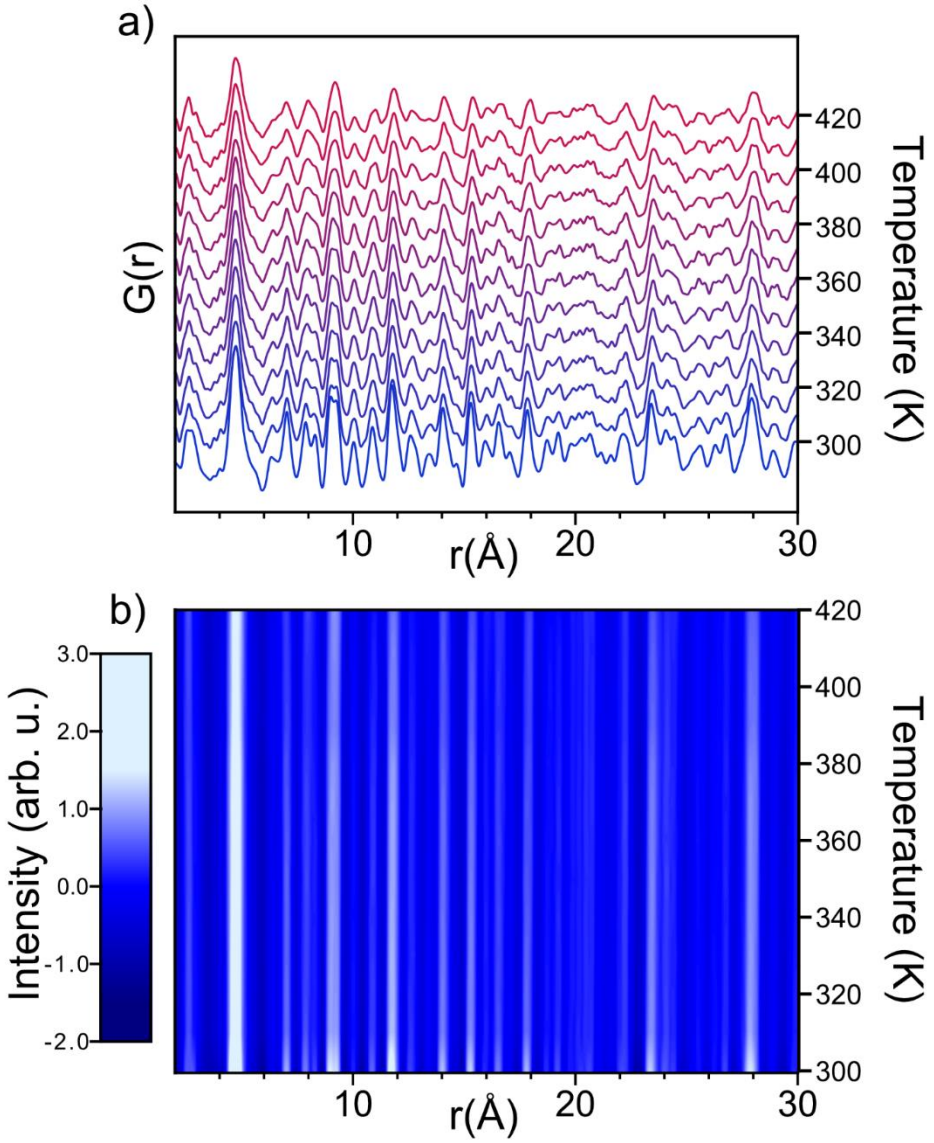

Figure S12. (a) Variable temperature PDFs during *in situ* heating from 310 – 420 K for fully lithiated α-Ge ($Li_{3.75}Ge$). Intervals of 10 K and 10 minute holds at each temperature were used. (b) Corresponding false colormaps of the PDF data; a linear interpolation was used between measured data points.

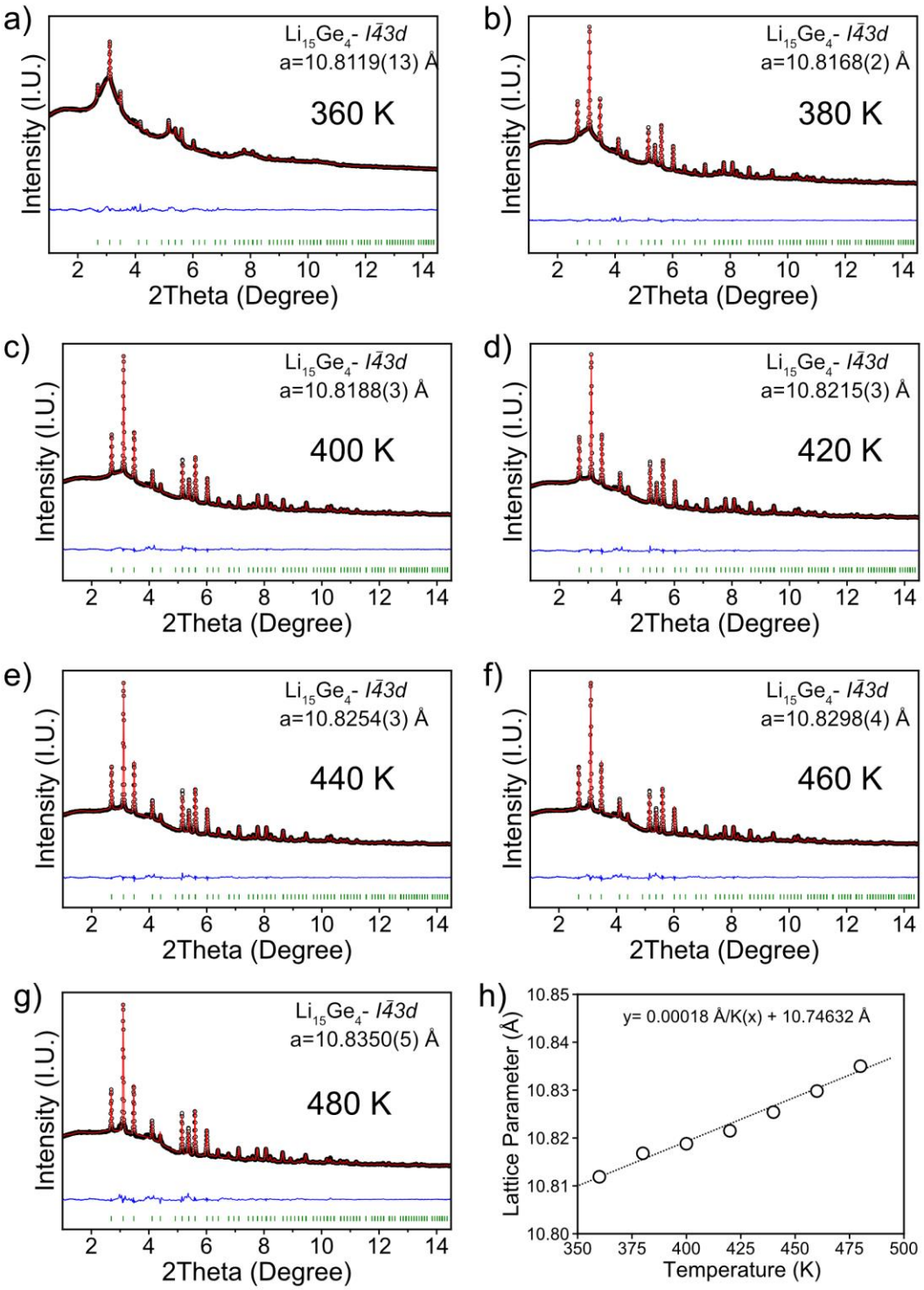

Figure S13. (a)-(g) Rietveld refinements of the XRD patterns obtained for $Li_{3.75}Ba_{0.19}Ge$ during *in situ* heating from 360 – 480 K; patterns were fit to the $Li_{15}Ge_4$ structural model; (h) Lattice parameter vs. temperature plot with a linear regression model.

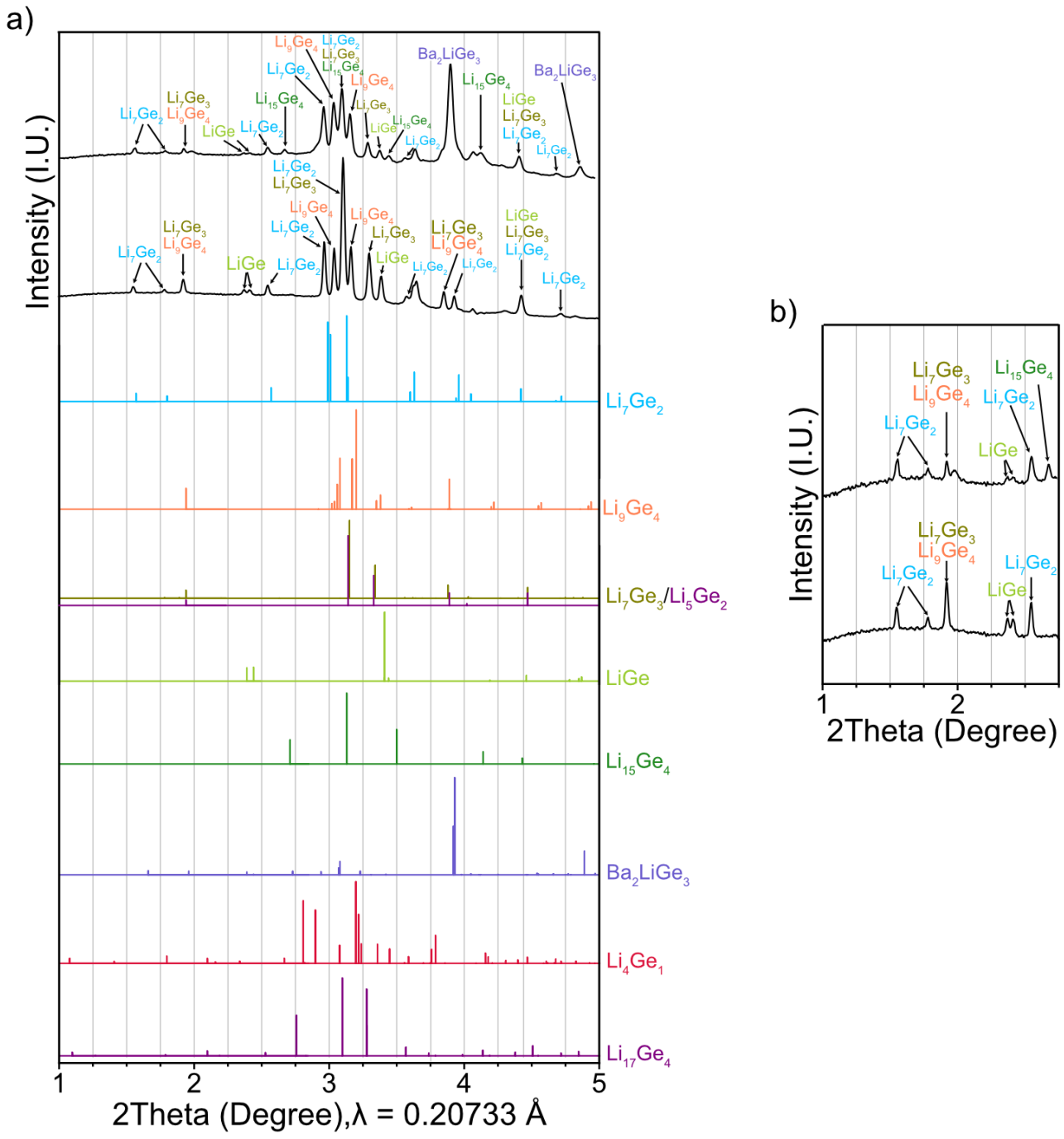

Figure S14. (a) XRD patterns of $Li_{3.75}Ba_{0.19}Ge$ and $Li_{3.75}Ge$ after heating to 480 K with the simulated XRD patterns of possible Li/Ge/Ba phases for identification. (b) Zoom in of the low angle peaks and their identification. The sources for the reference structures are included in Section 1.4 and 1.5 of the Supporting Information.

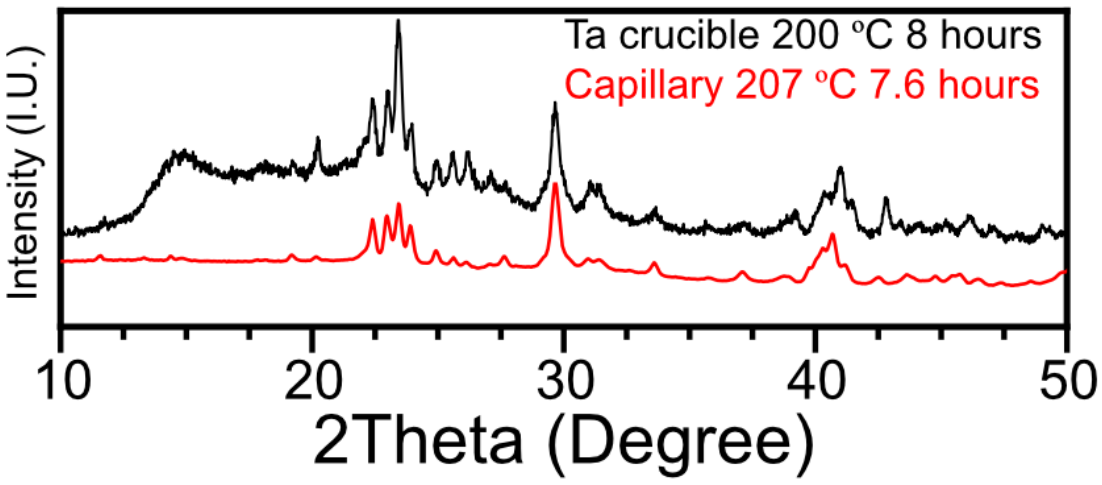

Figure S15. *Ex situ* laboratory powder XRD pattern of $Li_{3.75}Ba_{0.19}Ge$ after heating at 200 ºC for 8 hours under argon in a Ta boat (red) compared to the synchrotron *in situ* XRD heating pattern taken from $Li_{3.75}Ba_{0.19}Ge$ after heating at 480 K for 6.6 hours in a borosilicate capillary (black). Note that the XRD pattern for the sample heated in the Ta boat was taken at room temperature while the XRD pattern from the capillary was taken at 480 K (207 ºC). The background from $15 < 2\theta < 25$ in the black trace is from the Kapton film that was used to protect the sample from oxidation during the measurement. The similarity in the XRD patterns suggests that the use of the glass capillary in the synchrotron measurements did not have any effect on the formation of the reaction products.

Supporting Information References

(1) Dopilka, A.; Zhao, R.; Weller, J. M.; Bobev, S.; Peng, X.; Chan, C. K. Experimental and Computational Study of the Lithiation of $Ba_8Al_yGe_{46-y}$ Based Type I Germanium Clathrates. *ACS Appl. Mater. Interfaces* **2018**, *10*, 37981–37993.

(2) Juhás, P.; Davis, T.; Farrow, C. L.; Billinge, S. J. L. PDFgetX3: A Rapid and Highly Automatable Program for Processing Powder Diffraction Data into Total Scattering Pair Distribution Functions. *J. Appl. Crystallogr.* **2013**, *46*, 560–566.

(3) Yang, X.; Juhas, P.; Farrow, C. L.; Billinge, S. J. L. xPDFsuite: An End-to-End Software Solution for High Throughput Pair Distribution Function Transformation, Visualization and Analysis. arXiv:1402.3163 [cond-mat], **2014**.

(4) Farrow, C. L.; Juhas, P.; Liu, J. W.; Bryndin, D.; Boin, E. S.; Bloch, J.; Proffen, T.; Billinge, S. J. L. PDFfit2 and PDFgui: Computer Programs for Studying Nanostructure in Crystals. *J. Phys. Condens. Matter* **2007**, *19*, 335219.

(5) Borkiewicz, O. J.; Shyam, B.; Wiaderek, K. M.; Kurtz, C.; Chupas, P. J.; Chapman, K. W. The AMPIX Electrochemical Cell: A Versatile Apparatus for in Situ X-Ray Scattering and Spectroscopic Measurements. *J. Appl. Crystallogr.* **2012**, *45*, 1261–1269.

(6) Osman, H. H.; Bobev, S. Synthesis, Structural Characterization and Chemical Bonding of $Sr_7Li_6Sn_{12}$ and Its Quaternary Derivatives with Eu and Alkaline Earth Metal (Mg, Ca, Ba) Substitutions. A Tale of Seven Li-Containing Stannides and Two Complex Crystal Structures. *Eur. J. Inorg. Chem.* **2020**, 1979–1988.

(7) Fukuoka, H.; Kiyoto, J.; Yamanaka, S. Superconductivity and Crystal Structure of the Solid Solutions of $Ba_{8-\delta}Si_{46-x}Ge_x$ ($0 \leqslant x \leqslant 23$) with Type I Clathrate Structure. *J. Solid State Chem.* **2003**, *175*, 237–244.

(8) Smakula, A.; Kalnajs, J. Precision Determination of Lattice Constants with a Geiger-Counter X-Ray Diffractometer. *Phys. Rev.* **1955**, *99*, 1737.

(9) Hopf, V.; Müller, W.; Schäfer, H. Die Kristallstruktur Der Phase Li_9Ge_4. *Zeitschrift für Naturforsch.* **1970**, *25b*, 653.

(10) Hopf, V.; Müller, W.; Schäfer, H. Die Strucktur Der Phase Li_7Ge_2. *Zeitschrift für Naturforsch.* **1972**, *27b*, 1157–1160.

(11) Johnson, Q.; Smith, G.S.; Wood, D.W. The Crystal Structure of $Li_{15}Ge_4$. *Acta Crystallogr.* **1965**, *18*, 131–132.

(12) Morris, A. J.; Grey, C. P.; Pickard, C. J. Thermodynamically Stable Lithium Silicides and Germanides from Density Functional Theory Calculations. *Phys. Rev. B - Condens. Matter Mater. Phys.* **2014**, *90*, 22–24.

(13) Petrícek, V.; Dušek, M.; Palatinus, L. Crystallographic Computing System JANA2006: General Features. *Zeitschrift für Kristallographie* **2014**, 229, 345–352.

(14) Menges, E.; Hopf, V.; Schäfer, H.; Weiss, A. Die Kristallstruktur von LiGe — Ein Neuartiger, Dreidimensionaler Verband von Element(IV)-Atomen. *Zeitschrift für Naturforschung B* **1969**, 24, 1351–1352.

(15) von Schnering, H. G.; Bolle, U.; Curda, J.; Peters, K.; Carrillo-Cabrera, W.; Somer, M.; Schultheiss, M.; Wedig, U. Hückel Arenes with Ten π Electrons: Cyclic Zintl Anions Si_6^{10-} and Ge_6^{10-} Isosteric to P_6^{4-} and As_6^{4-}. *Angew. Chem. Int. Ed.* **1996**, *35*, 984–986.

(16) Zeilinger, M.; Fässler, T. F. Structural and Thermodynamic Similarities of Phases in the Li–Tt (Tt = Si, Ge) Systems: Redetermination of the Lithium-Rich Side of the Li–Ge Phase Diagram and Crystal Structures of $Li_{17}Si_{4.0-x}Ge_x$ for x = 2.3, 3.1, 3.5, and 4 as Well as $Li_{4.1}Ge$. *J. Chem. Soc. Dalt. Trans.* **2014**, *43*, 14959–14970.